Landslide Susceptibility Mapping Using LiDAR Data: A Case Study of Khao Yai National Park, Thailand

Chaikaew, N.,[1] Kumsap, C.,[2] Wutthisakkaroon, C.[3] and Pimmasarn, S.[4]*
[1]School of Information and Communication Technology, University of Phayao, Thailand
E-mail: nakarin9@hotmail.com
[2]Defence Technology Institute (Public Organization), Ministry of Defence Office of the Permanent Secretary of Defence, Thailand, E-mail: Chamnan.k@dti.or.th
[3]GIS Co., Ltd., Thailand, E-mail: Chanakan.yh@gmail.com
[4]Division of Research Administration, University of Phayao, Thailand, E-mail: Siriruk.pim@gmail.com
**Corresponding Author*

DOI: https://doi.org/10.52939/ijg.v19i3.2597

Abstract
Landslide is the natural problem occur worldwide due to its geological features, climatic characteristics and human activities. With the help of a geographic information system (GIS) and the Analytic Hierarchical Process (AHP) method, this research attempts to develop a map of landslide susceptibility. During the present investigation, a total of ten landslide influencing factors including elevation, slope, curvature, aspect, topographic wetness index (TWI), land cover, lithology, precipitation, distance to the road and drainage, were examined for the present analysis. Using AHP, weights were applied to each factor. The weight over lay approach was used to create the landslide susceptibility map, which was then divided into five classes. According to the research findings of the susceptibility classes, 19.97% of the research 's area was highly susceptible, followed by 61.65% of low susceptible, 17.33% of moderate susceptible, 0.94% of high susceptible, and 0.12% of very high susceptible. The areas with extremely high landslide susceptibility are adjacent to a road system and have a steep slope. The amount of mean annual rainfall is high and lithology belonging to the Jurassic metasediments. The findings for this map showing the research area's vulnerability to landslides in Khao Yai National Park are useful for planners and decision-makers for slope management and future development projects in the area.

Keywords: Analytical hierarchical process, Geographic Information System, Landslide susceptibility, LiDAR, Satellite image

1. Introduction

Landslides are a risky natural occurrence that often occurs, causing serious environmental harm globally, including the damage of both lives and environment [1] and [2]. The moving of a massive amount of rock, soil, or debris down a slope is referred to as a landslide [3]. Although, landslide commonly occur in hilly and mountainous areas, it has been proved that there are numerous factors influenced their occurrence such as intense or prolonged rainfall, earthquake, slope erosion and anthropogenic [4] and [5]. It's important to map landslide susceptibility since it's necessary for good land use planning and decision-making and can help to limit the losses brought on by a landslide. However, reliability of landslide susceptibility maps still relies on several factors such as suitable approach, quality and availability of data and scale of areas. To date, there are three main approaches of constructing landslide susceptibility map consist of quantitative, qualitative and semi-quantitative [4] and [6]. Two widely used, and considered to be objective [6], methodologies are provided by quantitative approaches: deterministic and statistical methods [7]. On the other hand, qualitative approaches are considered as subjective because they are depend on decisions of experts [6] and [8]. To assess the susceptible areas using these approaches, the landslide index will be used to determine the areas susceptible to landslides with comparable geological and geomorphologic characteristics [9] and [10]. For the semi-qualitative approaches, they are comprised of some qualitative approaches that use weighting and rating [11] and [12] as the Analytic Hierarchical Process (AHP) method [13] and [14] and the Weighted Linear Combination (WLC) method [1] and [12]. Throughout the last decades, One of the better

methods for landslide susceptibility mapping is the Saaty technique (AHP) [13], which is still actively utilized by researchers across several areas [9] [15] and [16].

Since, factors and geographical information are essential for creating accurate landslide susceptibility maps. Therefore, choosing reliable and high-quality data is necessary. In previous researches, they indicated that the Digital Elevation Model (DEM) resolution and its derived factors are important factors influenced the quality and accuracy of landslide susceptibility assessment apart from land cover, weather conditions and geology. The results revealed that the fine resolution DEM provides a better accuracy of landslide susceptibility assessment [17] [18] and [19]. Nowadays, there are many sources of remote sensing technology which provide a different resolution and quality DEM such as 30–90 m Shuttle Radar Topographic Mission (STRM), 12.5 m Advanced Land Observation Satellite (ALOS) Phased Array type L-band Synthetic Aperture Radar (PALSAR) and Light Detection and Ranging (LiDAR) [18] and [20]. To obtain a high resolution and accurate DEM for the extraction of landslide conditioning factors, LiDAR remains the finest source of high-quality and exact 3D data [18] and [21].

Currently, the landslide susceptibility in the area of Khao Yai National Park using LiDAR has not yet been assessed and there is available of LIDAR in the research area. Thus, the purpose of this research is to apply LiDAR and sentinel-2 imagery with the implementation of the analytic hierarchy process (AHP) approach in the research area which located in Khao Yai National Park, Thailand. The ten factors were utilized including elevation, slope, curvature, aspect, TWI, land cover, lithology, precipitation, distance to the road and drainage. A geographic database was created once all factors were transformed to raster layers. The zonation for landslide susceptibility was then evaluated and created.

2. Study Area

The study area was located at latitude 14° 26′ N and longitude 101° 22′ E in the middle of Khao Yai National Park, Thailand (**Figure 1)**. Thailand's first national park, Khao Yai, was created in 1962. The elevation above mean sea level ranges from 650 to 870 m. The mean annual precipitation has been approximately 2200 mm, and the mean annual temperature was around 22°-23°. May through October is the wet season, whereas November through April is the dry season [22]. Before to the park's establishment, certain sections were utilized for habitation and low-intensity agricultural work [22]. Therefore, this area consists of old-growth forests, secondary forest and grass land.

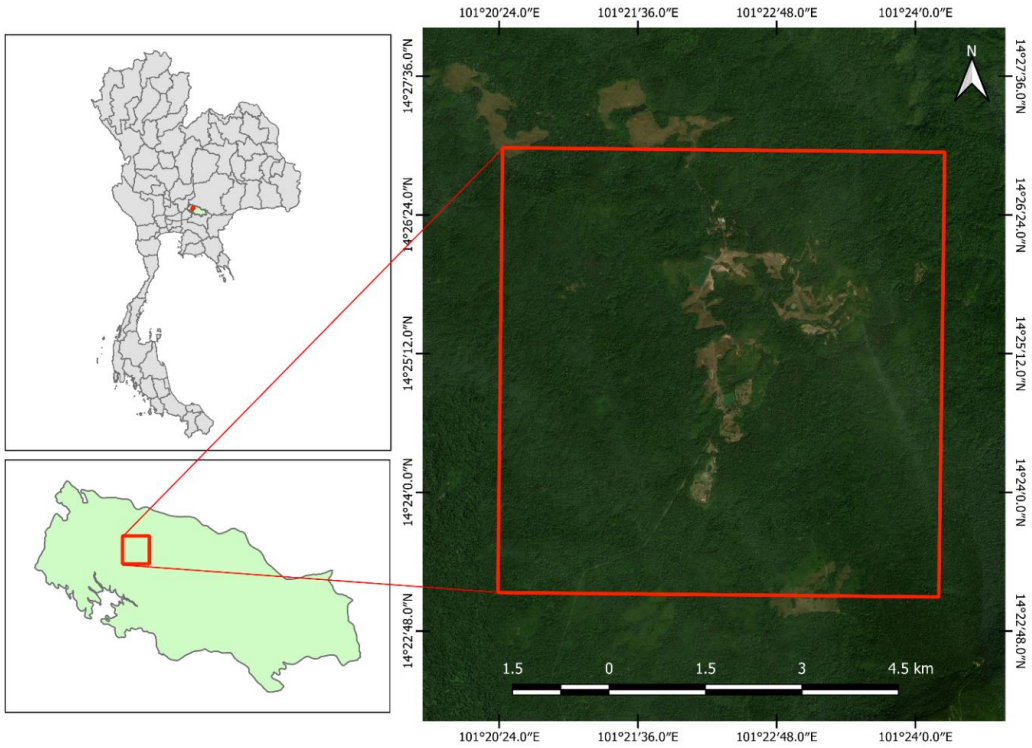

Figure 1: Map of the study area in Thailand's Khao Yai National Park

3. Data and Methods

3.1 Data Source

In this research, ten factors influencing landslide susceptibility comprise digital elevation model (DEM), slope, aspect, curvature, TWI, Land cover, lithology, distance from the road, distance from drainage and precipitation. To derive a DEM from LiDAR (LiDAR-DEM) and its derived factor, on April 10, 2017, the aerial laser scanning (ALS) program collected LiDAR data across about 64 km^2 (**Figure 1**). Land cover data was obtained from Sentinel-2 images of the study area. The Sentinel-2 data was downloaded on 23 December 2017 from https://scihub.copernicus.eu, to reflect the current land use pattern. Lithology data were derived from Department of Mineral Resources. Distance from road data with a 1:50000 scale geological map and distance from drainage data were derived from Ministry of Transport. Information on precipitation was obtained from the Thai Meteorological Department (TMD). To produce the precipitation intensity map of the study area, the Inverse Distance Weighting (IDW) interpolation method was applied.

3.2 Methodology

3.2.1 Preparation of landslide factor layers

To map landslides prone areas, ten factors which are elevation, slope, aspect, curvature, TWI, land cover, lithology, distance from the road, distance from drainage and precipitation were considered in this research according to previous research. To prepare each factor, elevation was the first factor that was considered in the susceptibility mapping. This factor has a great importance in landslide susceptibility regarding to the change in elevation of the surface area. Elevation used in this research was derived from LiDAR-derived DEM which was extracted using a k-nearest neighbour kriging method implemented in the LidR R package [23]. Furthermore, the DEM at 1 m resolution was used to extract other factors such as slope, aspect, curvature, TWI. To apply in landslide susceptibility, elevation was classified into seven classes including less than 700 m, 700-800 m, 800-900 m, 900-1000 m, 1000-1100 m, 1100-1200 m and more than 1200 m (**Figure 2a**).

Slope is an information identifying the degree of steepness of the location which varies from gentle to steep [10] and [24]. Mostly, steep slopes are expected to have higher susceptibility to landslide than gentle slopes [25]. In order to create the slope layer, LiDAR-DEM was extracted through SAGA and R programming. The slope data were classified into five classes as 0-10°, 10-20°, 30-40° and >40° (**Figure 2b**). Aspect is the data that displays terrain slope direction, measured clockwise in degrees from 0 to 360. By subjecting the surface to direct sunshine and/or intense rain, this factor regulates terrain processes and conditions such as soil hydration, plant cover, and soil thickness [25] and [26]. To create the aspect, the LiDAR-DEM was extracted and classified into nine classes consisting of flat, North (N), Northeast (NE), East (E), Southeast (SE), South (S), Southwest (SW), West (W) and Northwest (NW) (**Figure 2c**).

Curvature is the data that depict the topography's morphology [27]. In that cell, upwards convex surfaces have positive curvature values, whereas upwardly concave surfaces have negative curvature values. Areas with zero values are flat [28]. Concave, flat, and convex were the three categories into which the research 's curve data were divided (**Figure 2d**). TWI is a factor that indicated the moisture conditions at any point in a basin [29]. Using the RSAGA package in R programming, TWI was calculated using the DTM as the main attribute. The slope angle and specific catchment area (SCA), which is taken into account as the component that indicates the area's inclination to accept water, were combined to compute TWI. As seen below, the TWI equation is calculated [30]:

$$\text{TWI} = \ln\left(\frac{SCA}{tan\emptyset}\right) \qquad \text{Equation 1}$$

where SCA stands for the particular catchment area, ln for the natural algorithm, and φ for the slope angle. In this landslide susceptibility analysis, this data was classified into three classes comprising of less than 5 (Low), 5-10 (Moderate) and more than ten (High) (**Figure 2e**). Land cover represents the data which reflects the current land use pattern. In this research, Sentinel-2 images and field orthophoto map were used to generate land use using supervised classification in GIS software, and classified into three classes, namely dense forest, sparse forest and, settlement, and Barren, grassland and water body (**Figure 2f**).

One of the most important contributing variables for landslides is lithology since various lithological qualities show varying susceptibility to landslides. The lithology map indicates that the research area is covered by two separate lithological categories, which include Jurassic metasediments (Jpk) and, Permian and Trassic meta-volcanics and igneous rock (PTrv). Therefore, the lithology map was classified into two classes of Jpk and PTrv as illustrated in **Figure 2g**.

Distance from drainage that is another crucial factor in landslide development. This factor may increase river bank collapse while lowering the

slope's rock strength [24]. For this present research, Euclidean distance approach was used to construct six distinct buffers: 0-200 m, 200-400 m, 400-600 m, 600-800 m, 800-1000 m, and more than 1000 m (**Figure 2h**).

One of the main anthropogenic factors influencing the incidence of landslides is distance from the road [9]. Extensive constructions and deforestation were conducted in the region in order to construct the road systems. These actions can significantly increase the chances of landslides occurring when combined with other natural variables like severe rainfall events. In this research, six different buffer zones were generated including 0-200 m, 200-400 m, 400-600 m, 400-600 m, 600-800 m, 800-1000 m and more than 1000 m (**Figure 2i**).

Precipitation is the main affecting factor for landslide incidences. The assumption predicts that regions with high annual precipitation averages will be more susceptible to landslides than areas with less annual precipitation averages. Based on the average yearly rainfall data from the previous year, the thematic layer of rainfall for this research has been created using the IDW interpolation method in a GIS system. This data was categorized into four classes for applying in this landslide susceptibility analysis which are 1400-1600 mm, 1600-1800 mm, 1800-2000 mm and more than 2000 mm (**Figure 2j**). Finally, for consistency and subsequent data processing, all of the data layers were rescaled to a resolution of 1 m. The influencing factors of the landslide susceptibility analysis in the research region were generated using QGIS software.

3.2.2 Analytic hierarchy process

The Saaty (1980) approach known as the "analytical hierarchy process" (AHP) was employed extensively in several studies, including landslide susceptibility assessments. By computing a weight for each factor, it was employed to analyze the influence of each influencing landslide factor and sub-factor. The AHP is a subjective method that relies on pairwise comparison to assign a weight to each component and sub-factor based on expert opinions in order to establish priority scales. To derived factor and sub-factor weights, a pairwise comparison matrix was initially used to build a hierarchy of decision considerations. Then, based on expert opinion, a relative relevance score ranging from 1 to 9 was assigned to each element or sub-factor, comparing it to every other factor. Pairwise comparison matrix scale is shown in **Table 1**. When the factor on the matrix's vertical axis is more important than the factor on its horizontal axis, the value ranges between 1 and 9, while in the opposite case it ranges between the reciprocals 1/2 and 1/9. Finally, an average weight for each factor was calculated which is illustrated in the **Table 2** and **3**.

The consistency ratio (CR) was originally calculated using the equation below (Equation 2) in order to evaluate the level of consistency of the factors that were received from expert judgments [13].

$$CR = \frac{CI}{RI}$$

Equation 2

Where, RI is random consistency index, and CI is the consistency index which can be calculated by Equation 3 as [13]:

$$CI = \frac{(\lambda_{max} - n)}{(n-1)}$$

Equation 3

Where, λ_{max} is the principal eigenvalue of the matrix and it is computed from the *pairwise* matrix and n is the numbers of influencing factors. According to Saaty, a satisfactory consistency level should be less than or equal to 0.1. The low consistency ratio shows that each factor's determined weight is acceptable.

Table 1: Scale and definition for the pairwise comparison in AHP (Saaty 1977) [31]

Value	Definition
1	Equally important
3	Slightly more important
5	Strongly important
7	Very strongly important
9	Absolutely important
2,4,6,8	Intermediate

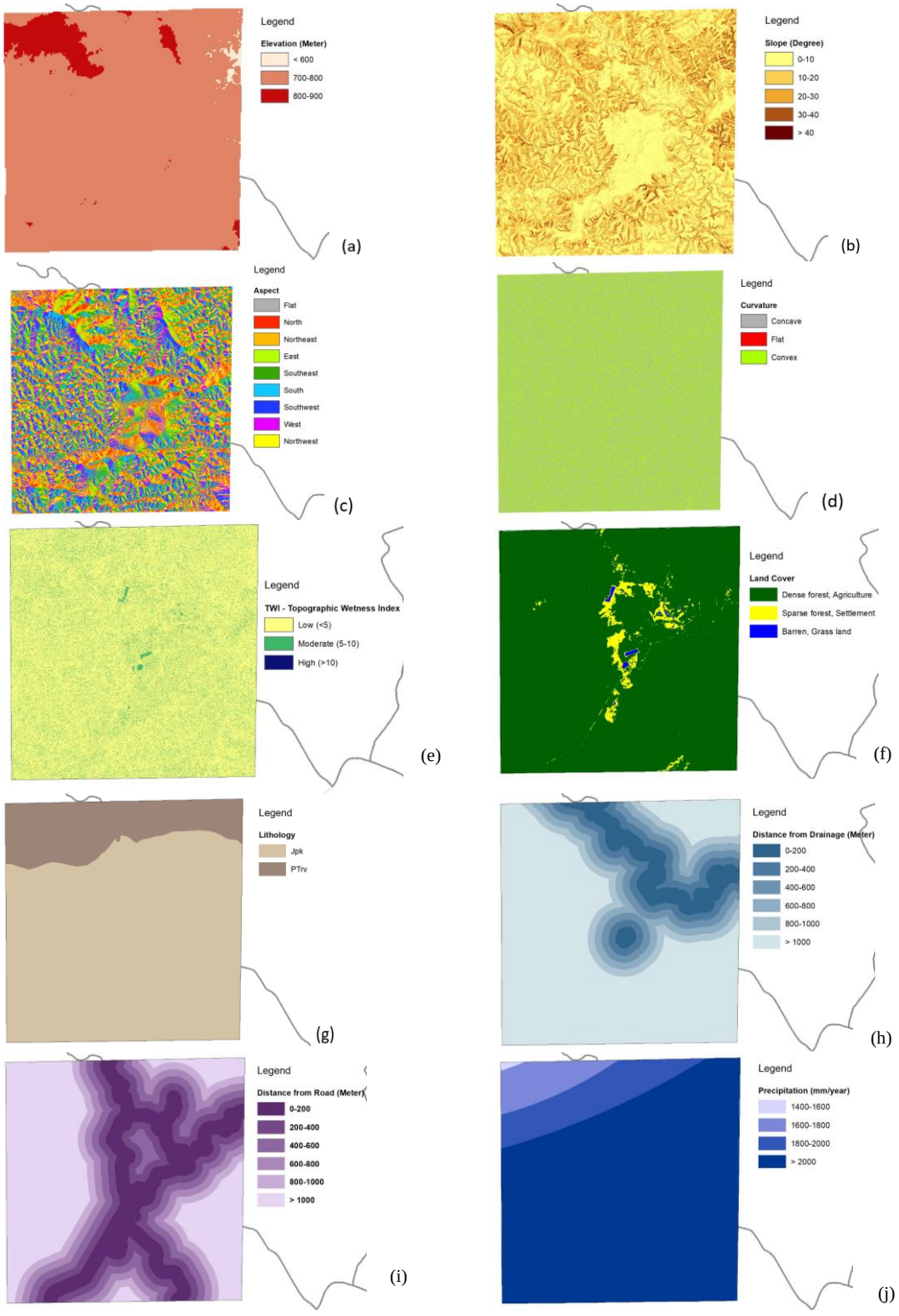

Figure 2: Ten factors utilized in this research (a) Elevation (b) Slope (c) Aspect (d) Curvature (e) TWI (f) Land cover (g) Lithology (h) Distance from the road (i) Distance from drainage (j) Precipitation

3.3.3 Landslide Susceptibility Index (LSI)

First, the appropriate weights for the different classes of factor layers were given to create the landslide susceptibility map. Then, all factor layers were generated to raster layers for the LSI assessment. The LSI of each pixel was then calculated using Equation 4 by integrating the weights of each component times the weight of the class [32].

$$LSI = \sum_{i=1}^{n} (W_i \times R_i)$$

Equation 4

where Wi and Ri are AHP derived weights, and influencing factors, respectively (**Tables 2 and 3**). Then, LSI values were classified into five classes to represent the area's five landslide susceptibility zone; namely, 1. very high (VH), 2. high (H), 3. moderate (M), 4. low (L) and 5. very low (VL) susceptibility zones (**Table 4**)

4. Results

In this research, the landslide susceptibility of the study area was mapped using a GIS-based AHP in Khao Yai National Park. For this area's landslide susceptibility analysis, ten landslide influencing factors i.e. slope, aspect, curvature, elevation, lithology, land use, distance to drainage, distance to the road, TWI and precipitation were utilized. Among the ten factors utilized to create the landslide susceptibility map, as shown in **Tables 2 and 3,** the factors and sub-factors' pairwise comparison matrix and relative weights were generated based on Saaty [13] approach. The factors as slope, precipitation and distance from the road showed high influence with a rating of 0.294, 0.195 and 0.165 respectively. The moderate influence factors were found in elevation, distance from drainage, lithology, aspect, land cover and curvature with a rating 0.075, 0.064, 0.059, 0.045, 0.040 and 0.035 respectively, while TWI found to be the lowest influencing factor with a rating of 0.027. In this research, the consistency ratio (CR) was calculated for all factors of the analysis was less that the cut-off value (0.1), indicting all factors that were used in this analysis is appropriate and reliable. So that, none were rejected from the analysis. Additionally, the weight factors determined for each class of a factor showed variable degrees of impacts both within and across the factors. In order to build the landslide susceptibility index (LSI) map, the weights derived for each factor were finally assigned to the corresponding factor classes. The equation of all factors integration for produce the LSI is shown below (Equation. 5)

LSI= Slope*0.294 + Precipitation *0.195 + Distance from the road*0.165
+ Elevation*0.075 + Distance from drainage*0.064
+ Lithology*0.059 + Aspect*0.045 + Land cover*0.040
+ Curvature*0.035 + TWI*0.027

Equation 5

Using the Equation (5), the LSI was computed. The finding is that the values of the landslide susceptibility index vary from 0.08 to 0.40. The landslide susceptibility index values corresponded to the relative susceptibility of a landslide to occur. As a result, the region was more prone to landslides the higher the rating. The LSI was divided into five classes using the natural break classifier based on the susceptibility index value: very low (VL), low (L), moderate (M), high (H), and very high (VH). This allowed researchers to better understand the spatial extent of different levels of landslide susceptibility in the research area. The LSI is displayed in **Figure 3** and **Table 4** displays the percentage of each susceptibility class's covered regions. The regions identified in **Figure 3** and **Table 4** as having a very high and high susceptibility to landslides, respectively, were 0.12% and 0.94% of the total area.

Table 2: Pairwise comparison matrix, factor weights and consistency ratio of landslide causative factors

Factors	(1)	(2)	(3)	(4)	(5)	(6)	(7)	(8)	(9)	(10)	Weight
(1) Slope	1	7	7	6	7	6	1	5	5	6	0.294
(2) Aspect	1/7	1	1/3	1	1/2	1/3	1/5	2	1/4	3	0.045
(3) Curvature	1/7	3	1	1/4	1/3	1	1/5	1/3	1/6	1	0.035
(4) Elevation	1/6	1	4	1	1/2	3	1/2	2	1/4	4	0.075
(5) Lithology	1/7	2	3	2	1	1	1/4	1	1/5	2	0.059
(6) Land cover	1/6	3	1	1/3	1	1	1/5	1/3	1/5	1	0.040
(7) Distance from road	1	5	5	2	4	5	1	3	1/3	5	0.165
(8) Distance from drainage	1/5	1/2	3	1/2	1	3	1/3	1	1/3	4	0.064
(9) Precipitation	1/5	4	6	4	5	5	3	3	1	5	0.195
(10) TWI	1/6	1/3	1	1/4	1/2	1	1/5	1/4	1/5	1	0.027
CR = 0.020											

Table 3: Classification of the landslide causative factors and their ranking classes based on the importance of each factor to landslide susceptibility

Criteria	Weight	Rank	CR
Slope (degree)	**0.294**	**1**	**0.054**
0-10	0.035	1	
10-20	0.068	2	
20-30	0.134	3	
30-40	0.260	4	
>40	0.503	5	
Precipitation (mm)	**0.195**	**2**	**0.012**
< 1200	0.056	1	
1200-1400	0.092	2	
1400-1600	0.114	3	
1600-1800	0.139	4	
1800-2000	0.233	5	
> 2000	0.366	6	
Distance from the road (m)	**0.165**	**3**	**0.038**
0-200	0.436	1	
200-400	0.237	2	
400-600	0.124	3	
600-800	0.083	4	
800-1000	0.072	5	
> 1000	0.048	6	
Elevation (m)	**0.075**	**4**	**0.069**
<700	0.045	7	
700-800	0.061	6	
800-900	0.070	5	
900-1000	0.215	2	
1000-1100	0.134	4	
1100-1200	0.163	3	
>1200	0.311	1	
Distance from drainage (m)	**0.064**	**5**	**0.052**
0-200	0.435	1	
200-400	0.224	2	
400-600	0.117	3	
600-800	0.088	4	
800-1000	0.076	5	
> 1000	0.059	6	
Lithology	**0.059**	**6**	**0.080**
JKpw	0.173	3	
Jpk	0.237	2	

PTrv	0.452	1	
Other	0.138	4	
Aspect	**0.045**	**7**	**0.066**
Flat	0.024	9	
North	0.030	8	
Northeast	0.048	7	
East	0.056	6	
Southeast	0.098	4	
South	0.269	1	
Southwest	0.240	2	
West	0.142	3	
Northwest	0.094	5	
Land cover	**0.040**	**8**	**0.056**
Dense forest, Agriculture	0.074	3	
Sparse forest, Settlement	0.283	2	
Barren, Grass land	0.643	1	
Curvature	**0.035**	**9**	**0.070**
Concave	0.649	1	
Flat	0.057	3	
Convex	0.295	2	
TWI - Topographic Wetness Index	**0.027**	**10**	**0.057**
Low (< 5)	0.083	1	
Moderate (5-10)	0.193	2	
High (> 10)	0.724	3	

Table 4: Landslide susceptibility classes derived from the LSI classification

Landslide susceptibility classes	LSI values	Area (km^2)	Area (%)
Very low	0.08 – 0.14	9.44	19.97
Low	0.15 – 0.21	29.15	61.65
Moderate	0.22 – 0.27	8.19	17.33
High	0.28 – 0.34	0.44	0.94
Very high	0.35 – 0.40	0.06	0.12
Total			100

The middle part of the research region has the greatest and highest landslide susceptibility zones, according to the landslide susceptibility map. These regions were not only distinguished by their proximity to road systems, drainage systems, and steep slopes. Additionally, these areas had the highest annual mean rainfall. For the lowest landslide susceptibility zones, the major areas were found in the northwest part of the research area. These areas were characterized with the gentle slope and distance from the road and drainage network more than 1000 m. The mean annual rainfall area represented the lowest amount (<1800 mm).

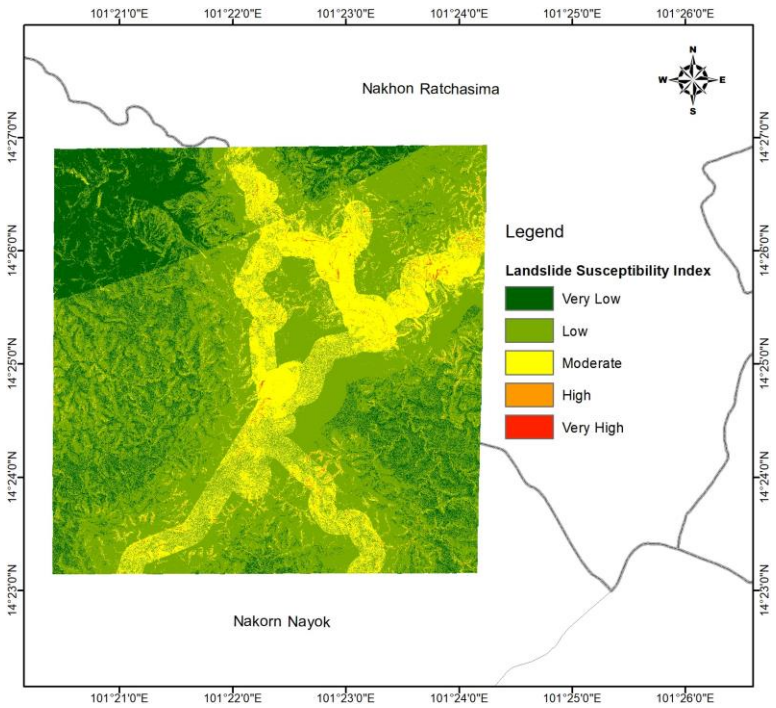

Figure 3: Landslide susceptibility map of the study area

5. Discussion

Landslide susceptibility mapping is still interesting among researchers and governments departments worldwide [33]. To produce a precise map of landslide susceptibility, it is well known that the quality of the DEM and their spatial resolution play an important role in various researches [18] and [32]. Thus, the high spatial resolution of DEM derived from LiDAR was considered with the implementation of the AHP approach to map landslide susceptibility in the research area situated in Khao Yai National Park, Thailand. Ten landslide affecting factors were utilized to determine susceptibility as slope, aspect, curvature, elevation, lithology, land cover, distance to drainage, distance to the road, precipitation and TWI. As the AHP approach, the factors and sub-factors were compared pairwise by expert judgment and CR was computed to assess the quality of consistency. The CR results was less than 0.1 which mean all factors and sub-factors are weighted reliably and suitably for applying in this research. From the results in **Tables 2** and **3**, slope is the main factor determining the occurrence of landslides followed by precipitation and distance from road. These finding are similar with other previous researches in various areas [9] [33] and [34]. Based on this research, the research area in Khao Yai National Park's landslide susceptibility map was divided into 5 susceptibility regions (**Figure 3**). Low susceptibility is the class with the greatest area, followed by very low, moderate, high, and very high (**Table 4** and **Figure 3**). The research area's center, which has a steep slope, a high mean annual precipitation, and is close to the road, has the highest and most susceptible parts. Furthermore, it was discovered that the majority of earlier landslide accidents in Khao Yai National Park took place along to roads with steep slopes during the rainy season. Similarly, Du et al., [36] and Akinci et al., [37] reported that the majority of landslide incidents occur near roads, particularly on hillsides with steep slopes. This implies that the first 3 influencing landslide factors are significant and reasonable for assessing the landslide susceptibility areas.

However, this research was limited by the lack of the historical landslides data in the research region for validation. Additionally, this is the first landslide susceptibility map in the research area using LiDAR-DEM and its derived factors due to a lack of publicly available LiDAR data. Thus, this research provided a fine detail of landslide susceptibility map and some derived factors from LiDAR data which can be used for further analysis. Moreover, the landslide susceptibility map can be a primary information in the research area for investigating and monitoring of areas prone to landslides.

6. Conclusions

The mapping of landslide susceptibility is essential for land use planning, disaster prevention, and reduction, particularly in the mountainous areas. Nowadays, there are a lot of studies on landslide susceptibility mapping. There are, however, few studies that use LiDAR-DEM, a high resolution and accurate DEM, to identify landslide-prone regions. Moreover, the DEM derived from LIDAR often used to obtain the most significant causative factors (e.g., slope, aspect, curvature and TWI). Therefore, a map of landslide susceptibility utilizing LiDAR-DEM and the AHP approach has been created in Khao Yai National Park. In this research, ten causative factors were utilized to assess the landslide susceptibility areas including slope, aspect, curvature, elevation, lithology, land cover, distance from drainage, distance from road, precipitation and TWI. Through all these factors, slope, distance from road and precipitation are the most crucial factors in this study. The landslide susceptible areas were subdivided into five classes as very low, low, moderate, high and very high classes with an area of 19.97%, 61.65%, 17.33%, 0.94% and 0.12% respectively. Most of the high and very high susceptibility area were found in the place where that have steep slope with distance from road less than 200 m, and the mean annual rainfall higher than 2000 mm. Therefore, such landslide susceptibility map is helpful for planners and decision makers for future land-use planning and landslide risks prevention planning in the research area.

Funding

This study was supported by funding from the Defence Technology Institute (DTI), Thailand.

Acknowledgements

The authors are grateful to the Department of National Parks, Wildlife and Plant Conservation (DNP), the Department of Mineral Resources and the Thai Meteorological Department for providing the valuable data. We also sincerely acknowledge the University of Phayao for the assistance in facilitating this research.

References

[1] Abay, A., Barbieri, G. and Woldearegay, K., (2019). GIS-based Landslide Susceptibility Evaluation Using Analytical Hierarchy Process (AHP) Approach: The Case of Tarmaber District, Ethiopia. *Momona Ethiop. J. Sci.*, Vol. 11(1). https://doi.org/ 10.4314/mejs.v11i1.2.

[2] Piralilou, S. T., Shahabi, H., Jarihani, Ben., Ghorbanzadeh, O., Blaschke, T., Gholamnia, K., Meena, S. R. and Aryal, J., (2019). Landslide Detection Using Multi-Scale Image Segmentation and Different Machine Learning Models in the Higher Himalayas. *Remote Sens.*, Vol. 11, 1–26. https://doi.org/10.3390/rs11212575.

[3] Cruden, D. M., (1991). A Simple Definition of a Landslide. *Bull. Int. Assoc. Eng. Geol.*, Vol. 43, 27–29.

[4] Westen, C. J., Castellanos, E. and Kuriakose, S. L., (2008). Spatial Data for Landslide Susceptibility, Hazard, and Vulnerability Assessment: An Overview. *Eng Geol*, Vol. 102(3–4), 112–131. https://doi.org/10.1016/j.enggeo.2008.03.010.

[5] Wubalem, A. and Meten, M., (2020). Landslide Susceptibility Mapping Using Information Value and Logistic Regression Models in Goncha Siso Eneses Area, Northwestern Ethiopia. *SN Appl. Sci.*, Vol. 2, (5), 1–19. https://doi.org/10.1007/s42452-020-2563-0.

[6] Guzzetti, F., Carrara, A., Cardinali, M. and Reichenbach, P., (1999). Landslide Hazard Evaluation: A Review of Current Techniques and their Application in a Multi-Scale Study, Central Italy. *Geomorphology*, Vol. 31, 181–216.

[7] Aleotti, P. and Chowdhury, R., (1999). Landslide Hazard Assessment: Summary Review and New Perspectives. *Bull. Eng. Geol. Environ.*, Vol. 58, 21–44. https://doi.org/10. 1007/s100640050066.

[8] Pradhan, B., Chaudhari, A., Adinarayana, J. and Buchroithner, M. F., (2012). Soil Erosion Assessment and its Correlation with Landslide Events Using Remote Sensing Data and GIS: A Case Study at Penang Island, Malaysia. *Environ. Monit. Assess.*, Vol. 184(2), 715–727. https://doi.org/10.1007/s10661-011-1996-8.

[9] Jazouli, A. E., Barakat, A. and Khellouk, R., (2019). GIS-multicriteria Evaluation Using AHP for landslide Susceptibility Mapping in Oum Er Rbia High Basin (Morocco). *Geoenvironmental Disasters*, Vol. 6(3), 1–12. https://doi.org/10.1186/s40677-019-0119-7.

[10] Psomiadis, E., Papazachariou, A., Soulis, K. X. and Alexiou, D. S., (2020). Charalampopoulos, I. Landslide Mapping and Susceptibility Assessment using Geospatial Analysis and Earth Observation Data. *Land*, Vol. 9(5). 1-26. https://doi.org/10.3390/land9050133.

[11] Achour, Y., Boumezbeur, A., Hadji, R., Chouabbi, A., Cavaleiro, V. and Bendaoud, E. A., (2017). Landslide Susceptibility Mapping Using Analytic Hierarchy Process and Information Value Methods along a Highway Road Section in

Constantine, Algeria. *Arab. J. Geosci.*, Vol. 10, 1–16. https://doi.org/10.1007/ s12517-017-2980-6.

[12] Ayalew, L., Yamagishi, H., Marui, H., and Kanno, T., (2005). Landslides in Sado Island of Japan: Part II. GIS-based Susceptibility Mapping with Comparisons of Results from Two Methods and Verifications. *Eng. Geol.*, Vol. 81(4). 432–445. https://doi.org/10.1016/j.enggeo.2005.08.004.

[13] Saaty, T. L., (1980). *The Analytic Hierarchy Process*, McGraw-Hill, Ed. New York, NY, USA: Scientific Research Publishing.

[14] Yacin, A., (2008). GIS-based Landslide Susceptibility Mapping Using Analytical Hierarchy Process and Bivariate Statistics in Ardesen (Turkey): Comparisons of Results and Confirmations. *Catena*, Vol. 72, 1–12. https://doi.org/10.1016/j.catena.2007.01.003.

[15] Devara, M., Tiwari, A. and Dwivedi, R., (2021). Landslide Susceptibility Mapping Using MT-InSAR and AHP Enabled GIS-based Multi-Criteria Decision Analysis. *Geomatics, Natural Hazards and Risk*, Vol. 12(1), 675–693. https://doi.org/10.1080/19475705.2021.1887939.

[16] Panchal, S. and Shrivastava, A. Kr., (2022). Landslide Hazard Assessment Using Analytic Hierarchy Process (AHP): A Case Study of National Highway 5 in India. *Ain Shams Eng. J.*, Vol. 13, 1–11. https://doi.org/10.1016/j.asej.2021.10.021.

[17] Brock, J., Schratz P., Petschko H., Muenchow, J., Micu, M. and Brenning, A., (2020). The Performance of Landslide Susceptibility Models Critically Depends on the Quality of Digital Elevation Models. *Geomatics, Natural Hazards and Risk*, Vol. 11(1), 1075–1092. https://doi.org/10.1080/19475705.2020.1776403.

[18] Chang, K. T., Merghadi, A., Yunus, A. P., Pham, B. T. and Dou, J., (2019). Evaluating Scale Effects of Topographic Variables in Landslide Susceptibility Models Using GIS-based Machine Learning Techniques. *Sci. Rep.*, Vol. 9(1), 1–21. https://doi.org/10.1038/s41598-019-48773-2.

[19] Gaidzik, K. and Ramírez-Herrera, M., (2021). The Importance of Input Data on Landslide Susceptibility Mapping. *Sci. Rep.*, Vol. 11, 1–14. https://doi.org/10.1038/s41598-021-98830-y.

[20] Rabby, Y. W., Ishtiaque, A. and Rahman Md. S., (2020). Evaluating the Effects of Digital Elevation Models in Landslide Susceptibility Mapping in Rangamati District, Bangladesh. *Remote Sens.*, Vol. 12(17), 1–35. https://doi.org/10.3390/rs12172718.

[21] Jaboyedoff, M., Oppikofer, T., Abellán, Antonio., Derron, M. H., Loye, A., Metzger, R. and Pedrazzini, A., (2012). Use of LIDAR in Landslide Investigations: A Review. *Nat Hazards*, Vol. 61, 5–28. https://doi.org/10.1007/s11069-010-9634-2.

[22] Brockelman, W. Y., Nathalang, A. and Gale, G. A., (2011). The Mo Singto Forest Dynamics Plot, Khao Yai National Park, Thailand. *Nat. Hist. Bull. Siam Soc.*, Vol. 22(57), 35–56.

[23] Roussel, J. R. and Auty, D., (2017). lidR: Airborne LiDAR Data Manipulation and Visualization for Forestry Applications, R package version 1.5.0, 2017.

[24] Zhao, Z., Liu, Z. Y. and Xu C., (2021). Slope Unit-Based Landslide Susceptibility Mapping Using Certainty Factor, Support Vector Machine, Random Forest, CF-SVM and CF-RF Models. *Front. Earth Sci.*, Vol. 9, 1–16. https://doi.org/10.3389/feart.2021.589630.

[25] Vijith, H. and Dodge-Wan, D., (2019). Modelling Terrain Erosion Susceptibility of Logged and Regenerated Forested Region in Northern Borneo through the Analytical Hierarchy Process (AHP) and GIS Techniques. *Geoenvironmental Disasters*, Vol. 6(8), 1–18. https://doi.org/10.1186/s40677-019-0124-x.

[26] Kouli, M., Loupasakis, C., Soupios, P. and Vallianatos, F., (2010). Landslide Hazard Zonation in High-Risk areas of Rethymno Prefecture, Crete Island, Greece. *Nat. Hazards*, Vol. 52(3), 599–621. https://doi.org/10.1007/s11069-009-9403-2.

[27] Fischer, J. T., Kowalski, J. and Pudasaini, S. P., (2012). Topographic Curvature Effects in Applied Avalanche Modeling. *Cold Reg. Sci. Technol.*, Vol. 74, 21–30. https://doi.org/10.1016/j.coldregions.2012.01.005.

[28] Alkhasawneh, M. S., Ngah, U. K., Tay, L. T., Isa, M., Ashidi, N. and Al-batah, M. S., (2013). Determination of Important Topographic Factors for Landslide Mapping Analysis Using MLP network. *Bull. Eng. Geol. Environ.*, Vol. 58, 21–44. https://doi.org/10.1155/2013/415023.

[29] Grabs, T., Seibert, J., Bishop, K. and Laudon, H., (2009). Modeling Spatial Patterns of Saturated Areas: A Comparison of the Topographic Wetness Index and a Dynamic Distributed Model. *J. Hydrol.*, Vol. 373, 15–23. https://doi.org/10.1016/j.jhydrol.2009.03.031.

[30] Mattivi, P., Franci, F., Lambertini, A. and Bitelli, G., (2019). TWI Computation: A Comparison of Different Open Source GISs. *Open Geospat Data Softw. Stand*, Vol. 4(6). https://doi.org/10.1186/s40965-019-0066-y.

[31] Saaty, T. L., (1977). A Scaling Method for Priorities in Hierarchical Structures. *J. Math. Psychol.*, Vol. 15, 234–281.

[32] Kumar, R. and Anbalagan, R., (2016). Landslide Susceptibility Mapping Using Analytical Hierarchy Process (AHP) in Tehri Reservoir Rim Region, Uttarakhand. *J. Geol. Soc. INDIA*, Vol. 87, 1–17. https://doi.org/10.1007/s12594-016-0395-8.

[33] Fell, R., Corominas, J., Bonnard, C., Cascini, L., Leroi, E. and Savage, W. Z., (2008). Guidelines for Landslide Susceptibility, Hazard and Risk Zoning for Land-Use Planning. *Eng. Geol.*, Vol. 102, 99–111. https://doi.org/10.1016/j.enggeo.2008.03.022.

[34] Mahalingam, R. and Olsen, M. J., (2016). Evaluation of the Influence of Source and Spatial Resolution of DEMs on Derivative Products Used in Landslide Mapping. *Geomatics, Natural Hazards and Risk*, Vol. 7(6), 1835–1855. https://doi.org/10.1080/19475705.2015.1115431

[35] Sonker, I., Tripathi, J. N. and Singh, A. K., (2021). Landslide Susceptibility Zonation Using Geospatial Technique and Analytical Hierarchy Process in Sikkim Himalaya. *Quaternary Science Advances*, Vol. 4, 1–17. https://doi.org/ 10.1016/j.qsa.2021.100039.

[36] Du, G., Zhang, Y., Iqbal, J., Yang, Z. and Yao, X., (2017). Landslide Susceptibility Mapping Using an Integrated Model of Information Value Method and Logistic Regression in the Bailongjiang Watershed, Gansu Province, China. *J. Mt. Sci.*, Vol. 1(2), 249–268.

[37] Akinci, H., Kilicoglu, C. and Dogan, S., (2020). Random Forest-Based Landslide Susceptibility Mapping in Coastal Regions of Artvin, Turkey. *Int. J. Geo-Inf.*, Vol. 9, 1–22. https://doi.org/0.3390/ijgi9090553